

Slow flows of yield stress fluids: Complex spatiotemporal behavior within a simple elastoplastic model

Guillemette Picard,¹ Armand Ajdari,¹ François Lequeux,² and Lydéric Bocquet^{3,*}

¹Laboratoire P.C.T., UMR CNRS 7083, ESPCI, 10 rue Vauquelin, 75005 Paris, France

²Laboratoire P.C.M., UMR CNRS 7615, ESPCI, 10 rue Vauquelin, 75005 Paris, France

³Laboratoire P.M.C.N., UMR CNRS 5586, Université Lyon I, 69622 Villeurbanne, France

(Received 23 June 2004; published 13 January 2005)

A minimal athermal model for the flow of dense disordered materials is proposed, based on two generic ingredients: local plastic events occurring above a microscopic yield stress, and the nonlocal elastic release of the stress these events induce in the material. A complex spatiotemporal rheological behavior results, with features in line with recent experimental observations. At low shear rates, macroscopic flow actually originates from collective correlated bursts of plastic events, taking place in dynamically generated fragile zones. The related correlation length diverges algebraically at small shear rates. In confined geometries, bursts occur preferentially close to the walls, yielding an intermittent form of flow localization.

DOI: 10.1103/PhysRevE.71.010501

PACS number(s): 83.50.-v, 81.40.Lm, 62.20.Fe

Many disordered dense systems exhibit a peculiar flowing behavior which strongly departs from the academic Newtonian description, with a shear rate dependence of the viscosity and indications of an actual yield stress value. For such “yield stress fluids,” it has been recognized recently that these *global* characteristics are, in most cases, associated with a peculiar *spatial* behavior, in the form of heterogeneous flow behavior, where a frozen region coexists with a flowing one (the so-called “shear band”). A striking remark is that such generic behaviors are observed in a wide class of experimental systems, with very different length/time/interaction scales, such as foams [1,2], granular systems [3,4], emulsions [3,5,6], colloidal glasses [7], and polymers, but also in simulations of granular systems, foams, and model glasses [8–11]. These generic features suggest an underlying common scenario for the flow properties, and has motivated various macroscopic phenomenological approaches (see, e.g., references cited in [5,8]). However, a consistent framework linking the global rheology to the local microscopic dynamics is still lacking, although some progress in this direction has been made in recent years [12–14]. In particular, studies have put forward the role of local plastic rearrangements in the global flow behavior [11,15,16]. Such an idea actually goes back to the Princen model for the deformation of foams [17]: flow occurs via a succession of reversible elastic deformations and irreversible plastic events (“T1” events in foams), associated with the existence of a local yield stress. However, if the corresponding physical picture seems *a priori* quite clear, a gap still persists between this simple microscopic scenario and the complex spatiotemporal organization responsible for the rheology of these materials at finite shear rates.

In this paper, we propose a simple mesoscopic model, constructed on the basis of two *minimal* and *generic* ingredients: localized plastic events associated with a microscopic yield stress, and the resulting elastic relaxation of the stress

over the system. We then show that the simplicity of the description contrasts with the complex rheological behavior deriving from it. In particular, we find the global rheology to be associated with a complex spatiotemporal organization which builds up as the system is sheared steadily, with an intermittent behavior corresponding to “bursts” of correlated events, the typical size of which diverges at small shear rate. We argue that in its present simple form our model seems to capture many observed experimental features and thus stands as a promising starting point for the elaboration of a generic scenario for the slow flow of yield stress fluids.

Let us now define the ingredients of our approach, which we implement here in the simplified frame of a two-dimensional (2D) scalar approach, focusing only on the simple shear components of the stress and strain. We consider a two-dimensional material to which an average shear rate $\dot{\gamma}$ is applied macroscopically (corresponding to a z -dependent displacement in the x direction). The material is described at a coarse-grained level, intermediate between the microscopic (particle) and macroscopic scale. The quantity of interest is the xz component of the time-dependent local shear stress $\sigma(x, z; t)$. First, without entering into details at this level, a few basic rules are stated: (i) below a (locally defined) yield stress σ_y , the system responds elastically to the imposed deformation; (ii) above σ_y , plastic events may occur in the system (along laws discussed in the following); (iii) plastic events take the form of a localized shear strain; (iv) such a plastic event induces a long-range *elastic* perturbation of the shear stress field in the material. A few remarks can be made at this level. First, although the notion of individual events is quite intuitive, in particular in foams, it has been evidenced unambiguously only recently at the microscopic level in disordered systems [11,16]. Second, the shear stress perturbation alluded to in (iv) is computed exactly within the framework of tensorial linear elasticity for an isotropic incompressible material as reported in Ref. [18]. This provides the explicit Green’s function, G_{xzx} , relating the stress variation, $\delta\sigma$, at any point in the system, to the xz component of the plastic strain $\epsilon^{pl}(\{x', z'\}; t)$, associated with

*Electronic address: lbocquet@lpmcn.univ-lyon1.fr

the plastic event localized at $\{x', z'\}$. Using the simpler notation G for this function yields

$$\delta\sigma(\{x, z\}; t) = 2\mu \int d\mathbf{r}' G(x, x', z, z') \epsilon^{pl}(\{x', z'\}; t). \quad (1)$$

The shear modulus μ has been exhibited for convenience. In a 2D infinite system, G decreases as $G(r) = 1/\pi r^2 \cos(4\theta)$ in cylindrical coordinates $\{r, \theta\}$ (in agreement with Refs. [16,19]). In general, its precise form depends on the specific geometry of the system: infinite, periodic, or confined between two rigid walls [18]. Summing up at this point, the evolution of the shear stress field results from the global elastic loading $\dot{\gamma}$ plus the perturbations induced by the localized plastic events,

$$\partial_t \sigma(\{x, z\}, t) = \mu \dot{\gamma} + 2\mu \int d\mathbf{r}' G(x, x', z, z') \dot{\epsilon}^{pl}(\{x', z'\}; t). \quad (2)$$

The last part of the modelization is the choice of a dynamical law for the plastic events, i.e., the feedback law relating the plastic relaxation $\epsilon^{pl}(\{x, z\}; t)$ to the stress field $\sigma(\{x', z'\}; t' < t)$. As in the Princen model, we choose a *local* relation with a threshold stress value σ_Y . In addition, an intrinsic time scale τ is introduced to describe the dynamics of the event. We anticipate that this will lead to a shear rate dependence of the dynamical structure in the flow, driving the system away from the critical quasistatic limit (self-organized criticality in a related quasistatic model was reported in [20]) to a more homogenous situation at large shear rate. Another important outcome is that the local stress may exceed the yield stress σ_Y for a finite time interval so that the averaged stress can also grow beyond this value, as observed experimentally.

There are actually many possibilities to introduce such an intrinsic time scale for plastic events, and few guides as to how we should do so. We make here a simple arbitrary choice and assume that the system locally alternates between a purely elastic state and a plastic state (during which stress is released), with *finite transition rates*: τ_{plast}^{-1} is the rate of transitions from *elastic to plastic*, while the reverse transition is characterized by a time τ_{elast} . Since plastic events only occur above the yield stress σ_Y , we take $\tau_{plast}(\sigma) = \infty$ if locally $\sigma < \sigma_Y$. We otherwise assume for sake of simplicity fixed values for the τ_{elast} and τ_{plast} , independent of the local stress. In order to finalize our model, we eventually have to quantify the amount of plastic strain released in an event and simply assume a Maxwell, viscoelasticlike relaxation of the material in the plastic state $\dot{\epsilon}_{plast} = \sigma/2\mu\tau$, with τ a mechanical relaxation time. All the previous discussion is best summarized by introducing a “state variable” $n(x, z)$ such that $n=0/1$ identifies the elastic/plastic state,

$$\dot{\epsilon}^{pl}(\{x, z\}, t) = \frac{1}{2\mu\tau} n(\{x, z\}, t) \sigma(\{x, z\}, t)$$

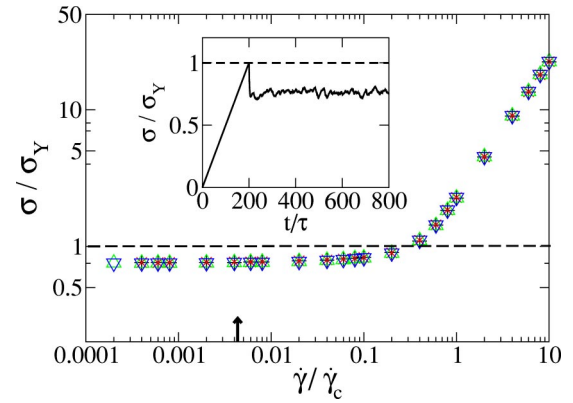


FIG. 1. Shear stress vs shear rate in units of σ_Y and $\dot{\gamma}_c = \sigma_Y/\mu\tau$ (log-log plot). The various symbols correspond to four different system sizes (from 4×4 to 32×32 blocks). Inset: time-dependent stress at the low shear rate corresponding to the arrow. The dashed line corresponds to the microscopic yield stress σ_Y .

$$n(\{x, z\}, t): \quad \begin{array}{cc} \tau_{plast}^{-1} & \tau_{elast}^{-1} \\ 0 \rightarrow 1 & 0 \leftarrow 1. \\ \text{if } \sigma > \sigma_Y & \forall \sigma \end{array} \quad (3)$$

Equations (2) and (3) constitute our minimal starting point to describe the dynamics of yield stress materials under flow. Note that, as in the somewhat related analysis of Langer [15], neither the stress nor the state variable are convected by the displacement field within the present simplified model. In other words, although the system locally flows (as described by a local shear rate), the net relative motion between the elements is neglected.

Before turning to their resolution, Eqs. (2) and (3) are made dimensionless using σ_Y and τ as stress and time units. An important point emerging from this procedure is that *the shear rate only appears in the form of the ratio $\dot{\gamma}/\dot{\gamma}_c$* , with $\dot{\gamma}_c = \sigma_Y/\mu\tau$. In this dimensionless form, our model therefore points out to a very general scenario, in which specific microscopic details are embedded in the precise values of σ_Y and $\dot{\gamma}_c$, as already suggested by some experiments [5,21].

The dynamical equations in this dimensionless form have been solved numerically by discretizing the material into blocks of elementary size a . A pseudospectral method is used, which allows us to express easily the stress increments in reciprocal space at each time step. On the other hand, the state variable $n(ia, ja)$ in the block $\{i, j\}$ evolves in real space according to the stochastic laws enounced above. We have focused on two geometries of $N = (L/a)^2$ blocks: a biperiodic geometry and a confined one, where the system is bounded by two rigid parallel walls. Practically, we have chosen $\tau_{plast} = \tau_{elast} = \tau$ for the results reported here.

We first quote the results for the biperiodic system. In Fig. 1, we plot the results for the macroscopic flow curve, which displays the essential features observed in experiments. First, a plateau is found at small shear rate, defining a *macroscopic yield stress* at vanishing shear rates, σ_Y^M . The latter is found to be smaller than the *microscopic* yield stress σ_Y , and also lower than the related peak value of the stress versus time at small shear rates (see inset in Fig. 1). A different regime is found at large shear rates, where a Newtonian behavior is

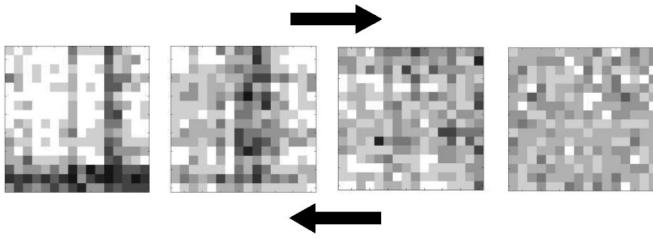


FIG. 2. Spatial distribution in $\{x, z\}$ plane of the cumulated plastic activity for a $N=16 \times 16$ system after $2N=512$ plastic events. From left to right the dimensionless shear rate, $\dot{\gamma}/\dot{\gamma}_c$, is $5.10^{-4}, 5.10^{-3}, 0.05, 2$. Gray levels correspond to the number of plastic events. Note that the occurrence of bursts of plastic activity in both (x and z) directions is due to the present *biperiodic* geometry. In the confined geometry where walls perpendicular to z are present, only bands parallel to x show up.

recovered. The dynamics of the time-dependent shear stress is also quite different in these two regimes. In particular, relative stress fluctuations around the mean value increase as the shear rate decreases (not shown), in agreement with observations in experiments and simulations [7,8]. A zoom on the dynamics at a shorter time scale actually shows that at small shear rate the stress exhibits successive periods of elastic raise and abrupt drops, as observed in the quasistatic limit in various systems [16]. These drops encompass many events, constituting “bursts” of correlated plastic activity. More interestingly these dynamically correlated events are also highly correlated in space, as emphasized in Fig. 2, where the spatial distribution of the cumulated plastic activity is plotted for a given succession of plastic events. This figure clearly shows that while at high shear rate plastic events are spatially decorrelated, a correlation pattern shows up as the shear rate is decreased, leading to the development of long-lived “fragile” zones in the system where nearly all the plastic activity takes place. This graph therefore suggests the development of a shear rate-dependent length scale in the system, which grows at small shear rates. In order to get more insight into this aspect, a possible route is to measure the length via measurements of correlation function. This is, however, a difficult task in general [22] and we have followed a different strategy here, analogous to finite-size scaling. Namely, since such a length is associated with the correlation of plastic events during a macroscopic stress drop, it should show up in the statistics of stress drops. To this end, we have computed the average amplitude of the drops of the global stress, $\Delta\sigma$, as a function of the applied macroscopic shear rate $\dot{\gamma}$ [23]. Results are shown in Fig. 3 for various system sizes. Let us first discuss the inset which exhibits the bare results for the average stress drop normalized by the average stress, $\Delta\tilde{\sigma}=\Delta\sigma(\dot{\gamma})/\sigma(\dot{\gamma})$. Three different regimes can be identified for all system sizes: two plateaus at large and small shear rates and an intermediate regime relating these two. We remark that the transition between the intermediate and “saturation” regime at low $\dot{\gamma}$ shifts to lower shear rates when the size of the system is increased. The system size dependence of this transition *at low shear rate* is best evidenced if one rescales the shear rates as $N\dot{\gamma}/\dot{\gamma}_c$, and the stress as $\Delta\tilde{\sigma}(\dot{\gamma})/\Delta\tilde{\sigma}(0)$, with $\Delta\tilde{\sigma}(0) \sim N^{-0.85}$ describing

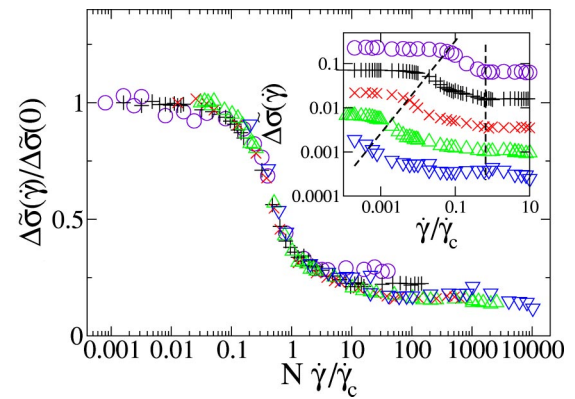


FIG. 3. Mean stress drop (normalized by the average stress), $\Delta\tilde{\sigma}$, as a function of the renormalized dimensionless shear rate, $N\dot{\gamma}/\dot{\gamma}_c$. Results in the inset are shown for five different sizes (from 2×2 to 32×32 blocks from top to bottom), while in the main graph all curves are rescaled using variables $\{N\dot{\gamma}/\dot{\gamma}_c, \Delta\tilde{\sigma}(\dot{\gamma})/\Delta\tilde{\sigma}(0)\}$ to emphasize the scaling of the transition between the small shear rate plateau and the intermediate regime. The dotted lines in the inset sketch the separation between the three dynamical regimes.

the low shear rate plateaus. This remarkable collapse of the rescaled curves suggest a quantification of the spatial correlations. Assuming the existence of a shear rate-dependent correlation length $\xi(\dot{\gamma})$ in the system, a saturation effect is expected for the mean stress drop when $\xi(\dot{\gamma})$ reaches the system size, $N^{1/2}a$. Note that we describe the correlations with a single diverging correlation length, in line with our observation that directions x and z are equivalent (see Fig. 2).

The rescaled graph indicates that such a saturation occurs for a fixed value of $N\dot{\gamma}/\dot{\gamma}_c$, which suggests $\xi(\dot{\gamma}) \sim \dot{\gamma}^{-\alpha}$, with $\alpha \approx 1/2$ from these data. Our model therefore explicitly yields indication of (at least) one *diverging length scale at small shear rates*, a feature absent in previous studies of yield stress fluids. Interestingly, the transition between the intermediate to the large shear rate regime on Fig. 3 (right dotted line in the inset) occurs roughly at the characteristic shear rate $\dot{\gamma}_c$, independent of system size, as for the macroscopic flow curve in Fig. 1. From these first results, our model yields a flow behavior with three different regimes as sketched on Fig. 4: (i) for $\dot{\gamma} > \dot{\gamma}_c$ (or $\sigma > \sigma_Y$), the blocks are uncorrelated in their dynamics and the flow is homogeneous; (ii) for $\dot{\gamma} < \dot{\gamma}_c$, correlations extend up to a correlation length $\xi(\dot{\gamma})$ which diverges algebraically at small shear rates; (iii) at very low shear rates, the correlation length saturates at the size of the system, leading to a quasistatic dynamical behavior.

We have also studied a confined geometry where two rigid walls bound the system in the z direction. A delicate technical point is then the calculation of the Green’s function, which shows that shear stress perturbation is amplified close to the walls [18]. Essentially, the picture in the confined geometry is very similar to that of the biperiodic system described above (Figs. 1, 3, and 4). One important specific feature, however, concerns the localization of the flow: while at high shear rate the flow is homogeneous, at low shear rates the plastic bursts occur preferentially close to the walls, and appear as spatially correlated structures that are parallel to

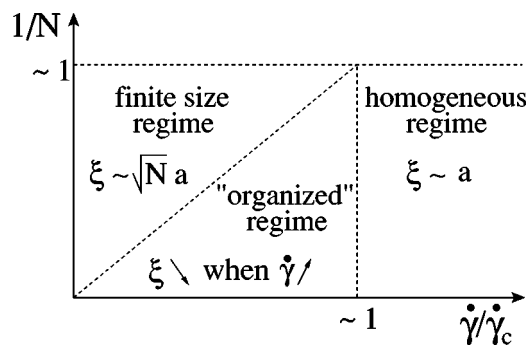


FIG. 4. Sketch of the emerging flow scenario in the $(\dot{\gamma}/\dot{\gamma}_c, 1/N)$ plane. Successive transitions from a homogeneous flow to an organized and a finite-size regime occur as the correlation length ξ grows from the block size to the system size, as the shear rate decreases.

the walls. In this last regime, the *average* flow corresponds to an increased shear rate close to the walls, but this “localization on average” of the flow is only part of a complex spatiotemporal pattern. A more detailed analysis of this regime is left for a future publication.

To sum up, we have proposed an athermal elastoplastic model for the flow of yield stress systems, constructed on the basis of two generic ingredients: localized plastic events, occurring above a microscopic yield stress with a finite dura-

tion, and an otherwise elastic behavior of the material (including redistribution of stress during the events). These two ingredients lead to a complex spatiotemporal behavior of the system at small shear rates. More precisely, a correlation length is exhibited which diverges at small shear rates, corresponding to intermittent collective events (correlated bursts of plastic events), leading to the creation of (long-lived) fragile zones where the deformation of the system takes place. These bursts take place preferentially close to the walls. At high shear rates, this correlation length is comparable to the size of the individual elements which flow independently from one another. These features are essentially compatible with recent observations in experimental or numerical systems: localization of the time-averaged deformation [1–5,8,9], intermittency at low shear rate [4,6,8,16], a diverging length scale at small shear rate in granular systems [24]. Moreover, numerical simulation of glassy systems [8] show that flow heterogeneities occur for global shear rates such that $\sigma < \sigma_Y$, a conclusion which is recovered within our minimal model. Although our model should be refined to take into account convection and the full tensorial nature of the problem, the present early results suggest that the generic behaviors observed in the experiments and molecular simulations originate in a minimal number of ingredients. This opens the possibility for a coherent and robust scenario for the slow flow behavior of disordered materials.

-
- [1] J. Lauridsen, G. Chanan, and M. Dennin, *Phys. Rev. Lett.* **93**, 018303 (2004).
 [2] G. Debrégeas, H. Tabuteau, and J.-M. di Meglio, *Phys. Rev. Lett.* **87**, 178305 (2001).
 [3] F. Da Cruz, F. Chevoir, D. Bonn, and P. Coussot, *Phys. Rev. E* **66**, 051305 (2002).
 [4] W. Losert, L. Bocquet, T. C. Lubensky, and J. P. Gollub, *Phys. Rev. Lett.* **85**, 1428 (2000).
 [5] P. Coussot *et al.*, *Phys. Rev. Lett.* **88**, 218301 (2002).
 [6] J.-B. Salmon, A. Colin, S. Manneville, and F. Molino, *Phys. Rev. Lett.* **90**, 228303 (2003).
 [7] F. Pignon, A. Magnin, and J.-M. Piau, *J. Rheol.* **40**, 573 (1996).
 [8] F. Varnik, L. Bocquet, J.-L. Barrat, and L. Berthier, *Phys. Rev. Lett.* **90**, 095702 (2003).
 [9] A. Kabla and G. Debrégeas, *Phys. Rev. Lett.* **90**, 258303 (2003).
 [10] V. V. Bulatov and A. S. Argon, *Modell. Simul. Mater. Sci. Eng.* **2**, 167 (1994).
 [11] M. L. Falk and J. S. Langer, *Phys. Rev. E* **57**, 7192 (1998).
 [12] L. Berthier, J.-L. Barrat, and J. Kurchan, *Phys. Rev. E* **61**, 5464 (2000).
 [13] J. C. Baret, D. Vandembroucq, and S. Roux, *Phys. Rev. Lett.* **89**, 195506 (2002).
 [14] A. Lemaître, *Phys. Rev. Lett.* **89**, 195503 (2002).
 [15] J. S. Langer, *Phys. Rev. E* **64**, 011504 (2001).
 [16] C. Maloney and A. Lemaître, *Phys. Rev. Lett.* **93**, 016001 (2004).
 [17] H. M. Princen, *J. Colloid Interface Sci.* **91**, 160 (1983).
 [18] G. Picard, A. Ajdari, F. Lequeux, and L. Bocquet, *Eur. Phys. J. E* **15**, 371 (2004).
 [19] J. D. Eshelby, *Proc. R. Soc. London, Ser. A* **241**, 376 (1957).
 [20] K. Chen, P. Bak, and S. P. Obukhov, *Phys. Rev. A* **43**, 625 (1991).
 [21] M. Cloître, R. Borrega, F. Monti, and L. Leibler, *Phys. Rev. Lett.* **90**, 068303 (2003).
 [22] L. Berthier, *Phys. Rev. Lett.* **91**, 055701 (2004).
 [23] Stress drops can be identified for a given duration of the time intervals δt : they start when the global stress decreases over a δt -long-time interval and ends at the first subsequent increase over an interval. We chose $\delta t = 0.01 \tau$ and checked that results plotted in Fig. 3 are robust with respect to variations of δt .
 [24] G. D. R. Midi, *Eur. Phys. J. E* **14**, 341 (2004).